

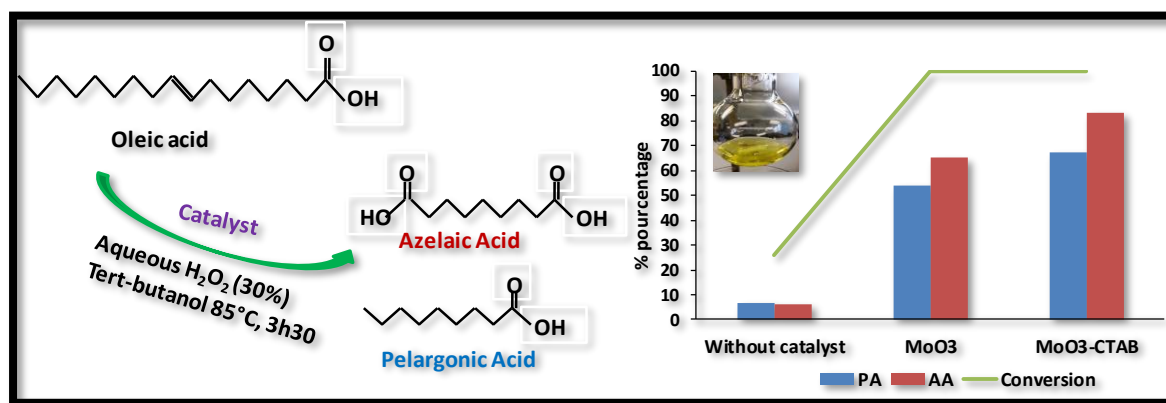
# Chapter 7. Sustainable oxidative cleavage of vegetable oils into diacids by organo-modified molybdenum oxide heterogeneous catalysts

Aimé Serge Ello<sup>1,2</sup>, Amir Enferadi-kerenkan<sup>1</sup>, Albert Trokourey<sup>2</sup>, Trong-on Do<sup>1\*</sup>

1. Department of Chemical Engineering, Laval University, Quebec, G1V 0A6, Canada.
2. Université Félix Houphouët-Boigny de Cocody, Laboratoire de Chimie Physique, 22 bp 582 Abidjan, Côte d'Ivoire.

*Journal of the American Oil Chemists' Society, 2017, 94, 1451-1461*

*Aimé Serge Ello and Amir Enferadi-kerenkan contributed equally to this work.*



## Résumé

L'exploitation d'huiles végétales pour produire des diacides d'une valeur industrielle via un processus respectueux de l'environnement nécessite un catalyseur efficace et recyclable. Dans ce travail, un nouveau système catalytique à base de trioxyde de molybdène organo-modifié a été synthétisé par une méthode hydrothermale verte en une seule étape, en utilisant de la poudre de Mo comme précurseur, du peroxyde d'hydrogène et des tensioactifs amphiphiles. comme agents de coiffage. Les matériaux synthétisés ont d'abord été caractérisés par différentes techniques comprenant XRD, SEM, TGA et FTIR. De manière intéressante, diverses morphologies ont été obtenues en fonction de la nature des agents tensioactifs et des conditions synthétiques. Les catalyseurs synthétisés ont été utilisés dans le clivage oxydatif de l'acide oléique, l'acide gras insaturé le plus abondant, pour produire des acides azélaïques et pélargoniques avec un oxydant bénin, H<sub>2</sub>O<sub>2</sub>. D'excellentes activités catalytiques conduisant à une conversion complète de l'acide oléique initial ont été obtenues, notamment pour l'oxyde de molybdène coiffé de CTAB (rapport molaire CTAB / Mo de 1: 3) qui ont respectivement donné 83 et 68% de production d'acides azélaïque et pélargonique. Ce sont les rendements les plus élevés obtenus jusqu'à présent pour cette réaction par des catalyseurs hétérogènes. De plus, le catalyseur coiffé de CTAB peut être commodément séparé du mélange réactionnel par simple centrifugation et réutilisé sans perte significative d'activité jusqu'à au moins 4 cycles.

## Abstract

Exploiting vegetable oils to produce industrially valuable diacids via an eco-friendly process requires an efficient and recyclable catalyst. In this work, a novel catalytic system based on organo-modified molybdenum trioxide was synthesized by a green hydrothermal method in one simple step, using Mo powder as precursor, hydrogen peroxide, and amphiphilic surfactants cetyltrimethylammonium bromide (CTAB) and tetramethylammonium bromide (TMA) as capping agents. The synthesized materials were, first, characterized by different techniques including XRD, SEM, TGA, and FTIR. Interestingly, various morphologies were obtained depending on the nature of the surfactants and synthetic conditions. The synthesized catalysts were employed in oxidative cleavage of oleic acid, the most abundant unsaturated fatty acid, to produce azelaic and pelargonic acids with a benign oxidant, H<sub>2</sub>O<sub>2</sub>. Excellent catalytic activities resulting in full conversion of initial oleic acid were obtained, particularly for CTAB-capped molybdenum oxide (CTAB/Mo molar ratio of 1:3) that gave 83 and 68% yields of production of azelaic and pelargonic acids, respectively. These are the highest yields that have been obtained for this reaction on heterogeneous catalysts up to now. Moreover, the CTAB-capped catalyst could be conveniently separated from the reaction mixture by simple centrifugation and reused without significant loss of activity up to at least 4 cycles.

## 7.1 Introduction

A Biomass-derived feedstock is one of the most promising candidates that would substitute the crude oil-based fuels and chemicals. The vast abundance and renewable nature of vegetable oils have attracted growing interest in both academic and industrial researches. Triglycerides are the main component of oleaginous feedstock, i.e. vegetable oils, the unsaturated fatty acids of which can be chemically modified, mainly through their double bonds, to be converted into value-added chemicals. For instance, oleic acid, the most abundant monounsaturated fatty acid [338], can produce a di- and a mono-carboxylic acids, azelaic and pelargonic acids, through oxidative cleavage reaction. These are valuable materials for different industrial applications like production of polymers, plasticizers, adhesives, lubricants, cosmetics, herbicides, fungicides etc. [2,4,1,5,3]. Currently, the oxidative cleavage of oleic acid is performed in industry via ozonolysis. However, using ozone is not in line with the principles of sustainable chemistry due to its inevitable hazardous problems. Attempting to employ a benign oxidant, several catalyst/oxidant systems, in homogeneous and heterogeneous forms, have been reported in the literature for oxidative cleavage of unsaturated fatty acids, which have been thoroughly reviewed in our recent review paper [91].

Homogeneous catalysts have generally shown excellent performances in oxidation of unsaturated fatty acids (e.g. production yield of azelaic acid up to 82% from oleic acid by peroxo complex, oxoperoxo (pyridine-2,6-dicarboxylato) molybdenum (VI) hydrate ( $\text{Mo}(\text{O}_2)[\text{C}_5\text{H}_3\text{N}(\text{CO}_2)_2](\text{H}_2\text{O})$ ) catalysts [3]), but such catalytic systems have been always associated with lack of catalyst recovery. On the other hand, activities of heterogeneous catalysts, with recovery ability, reported so far, are not as high as homogeneous ones [91,45]. Various strategies have been reported in the literature to improve the efficiency of the reaction, like reaction in supercritical fluids with dual oxidants and microwave irradiations and ultrasound-assisted reactions [339,384,58,57]. Works should be encouraged to find a suitable reaction strategy that enjoys both high activity and efficient recovery. Current efforts in this domain can be generally classified into two groups. The first group is involving different transition metal oxide catalysts, which are inherently solid, along with a benign oxidant such as hydrogen peroxide or sodium hypochlorite, and the second group is based on heterogenization of highly active homogeneous catalysts, like polyoxometallates, via immobilization or solidification methods [385,252,186,191]. In these two groups, direct or indirect

selective oxidative cleavage mechanisms have been proposed [386]. Nevertheless, an efficient heterogeneous catalytic system that can afford the excellent reaction yields obtained with the homogeneous catalysts has not been reported so far.

In this work, we have tried to extend the proved potential of molybdenum oxide as an oxidizing solid catalyst [387-389] to oxidative cleavage reaction of unsaturated fatty acids. Curiously, employing MoO<sub>3</sub> heterogeneous catalysts in oxidative cleavage of oleic acid has not been reported so far, to our knowledge. Herein, a series of molybdenum oxides were synthesized via simple oxidative dissolution of Mo powder in H<sub>2</sub>O<sub>2</sub>, with and without organic surfactants. Two well-known quaternary ammonium surfactants, cetyltrimethylammonium bromide (CTAB) and tetramethylammonium bromide (TMA) with different alkyl chain lengths were employed as capping agents. The effects of CTAB and TMA in different concentrations in the synthesis medium on physicochemical properties and morphology of the products, as well as enhancement of catalytic efficiency in the liquid phase oxidative cleavage of oleic acid by organo-modification of the surface of molybdenum oxide have been investigated.

## **7.2 Experimental**

### **7.2.1 Synthetic details**

Surfactant-capped molybdenum oxide particles were synthesized by hydrothermal method using molybdenum powder (99.9%, Alfa Aesar), hydrogen peroxide (30%, Fischer Scientific) and surfactants; CTAB (98%, Fischer Scientific), and TMA (98%, Aldrich). In a typical synthesis, 1 g of metallic molybdenum powder was added to 10 ml of deionized water and the mixture was stirred for 30 minutes at room temperature. Then, the mixture was placed in an ice bath under a well-ventilated fume hood. To this mixture, an aqueous solution of hydrogen peroxide was added dropwise under vigorous stirring until the color of the solution changed to yellow (attention: the reaction is very exothermic and must be done in an ice bath under skilled supervision). The determined amounts of surfactants (CTAB or TMA) to obtain surfactant/ molybdenum molar ratios of 1:2, 1:3, 1:4, were added to the yellow solution. The resultant slurry was refluxed at 100 °C for 4 hours. Finally, the solid product was separated by centrifugation at high speed and dried in air at 70 °C for 10 h.

## 7.2.2 Characterization equipment

The physicochemical properties of the materials were characterized by X-ray diffraction (XRD), Scanning electron microscopy (SEM), Thermo-gravimetric analysis (TGA) and Fourier transform infra-red spectroscopy (FT-IR). Powder X-ray diffraction (XRD) patterns of the samples were obtained on a Bruker SMART APEXII X-ray diffractometer equipped with a Cu K $\alpha$  radiation source ( $\lambda = 1.5418 \text{ \AA}$ ) with steps of  $0.02^\circ$  and step time of 1 second. Scanning electron microscopy (SEM) images were taken on a JEOL 6360 instrument at an accelerating voltage of 3 kV. Materials were spread on a carbon tape prior to analysis. The FT-IR spectra were recorded on an FTS 45 infrared spectrophotometer with the KBr pellet technique. Thermo-gravimetric analyses (TGA) were performed in the temperature range of 30 °C to 800 °C with a TGA Q500 V20.13 Build 39 thermo-gravimetric analyzer at a heating rate of 5 °C min<sup>-1</sup> under an air flow or argon flow of 50 mL min<sup>-1</sup>.

## 7.2.3 Catalytic test

Catalytic reactions were carried out in a glass reactor equipped with an oil bath, magnetic stirrer, and reflux condenser. Typically, the reactor was charged with a suspension of 0.4 g catalyst and 4 ml aqueous H<sub>2</sub>O<sub>2</sub>. Then, 1 g oleic acid ( $\geq 99\%$ , Sigma-Aldrich) was added dropwise under stirring followed by addition of 8 mL tert-butanol as solvent. The reaction mixture was heated to 85 °C and kept at this temperature for a reaction time of 3 h 30 min. After the reaction, the solution was allowed to cool down to room temperature. During the reaction, the system showed homogeneous catalysis properties, while upon cooling down at the end of reaction, the catalyst particles were precipitated, enabling self-separation performance. The precipitated catalyst was separated using a centrifuge at 8000 rpm and recovered via washing with ethanol and water several times and drying at 70 °C for 4 h, in order to be used in the next catalytic cycle. The resultant solution then underwent a derivatization process prior to GC-MS analysis.

## 7.2.4 Quantitative analysis of the product

Gas chromatography-mass spectrometry (GC-MS) was used for separation and quantification of methyl esters of fatty acids. Since fatty acids in their free forms are difficult to

analyze with GC (due to their adsorption issues on stationary phase in GC columns), the reaction products were esterified before GC-MS analysis via Metcalfe et al. derivatization procedure [334,335] using boron trifluoride solution in methanol. Briefly,  $\text{BF}_3$ -methanol (5 ml) (10% w/w, Sigma-Aldrich Co.) was added to the solution of products of the oxidation reaction. Then, the solution was heated to 80 °C for 15 min, followed by cooling down at room temperature for about 20 min. The esterified products were extracted by adding 3 ml petroleum ether and 2 ml water. The extraction was repeated for the aqueous phase (lower layer) twice. After dehydration by sodium sulfate and removal of the solvent by passing a steady stream of dry air, the obtained organic phase was ready for injection to GC-MS.

A typical derivatized sample including methyl esters of the involved fatty acids (expectedly dimethyl azelate, methyl pelargonate, and possibly methyl oleate) was injected to the GC-MS which had been previously calibrated by analytical standards of these methyl esters. The GC-MS system included a Hewlett-Packard HP 5890 series GC system and MSD Hewlett-Packard model 5970. The GC system was equipped with Zebron ZB-5MS capillary column (30 m  $\times$  0.25 mm  $\times$  0.25 mm). Helium was used as a carrier gas with the flow rate of 30 mL/min. A split ratio of 15:1 was fixed. The front inlet temperature was 280 °C. The oven temperature program consisted of maintaining at 50 °C for 2 min, then a ramp rate of 10 °C/min to 160 °C followed by a hold-up time of 1 min, and further increase at the rate of 5°C/min to 290 °C. Direct injection was employed with 1  $\mu\text{L}$  injection amount for each run, and the injection was repeated at least four times for each sample to be averaged. HP Chemstation software was used to analyze data.

## 7.3 Results and discussion

### 7.3.1 Characterization of the catalysts

The crystalline structures of the synthesized samples were analyzed by X-ray diffraction. Figure 7.1 represents the X-ray diffraction patterns of the synthesized molybdenum oxides. The sharp peaks indicate the good crystallinity of the products, which were synthesized even without using autoclave and in a short time. XRD pattern of the sample prepared without using any surfactant, denoted as MO, (Figure 7.1a) confirmed that it was composed of  $\text{MoO}_3\cdot\text{H}_2\text{O}$ , in accordance with PDF no. 26-1449 of ICDD library of spectra. The pattern exhibits 5 well-resolved peaks indexed (010), (100), (120), (020), (030) planes of triclinic molybdenum trioxide hydrate

material, and no peaks corresponding to other phases implies the single triclinic phase of this material.

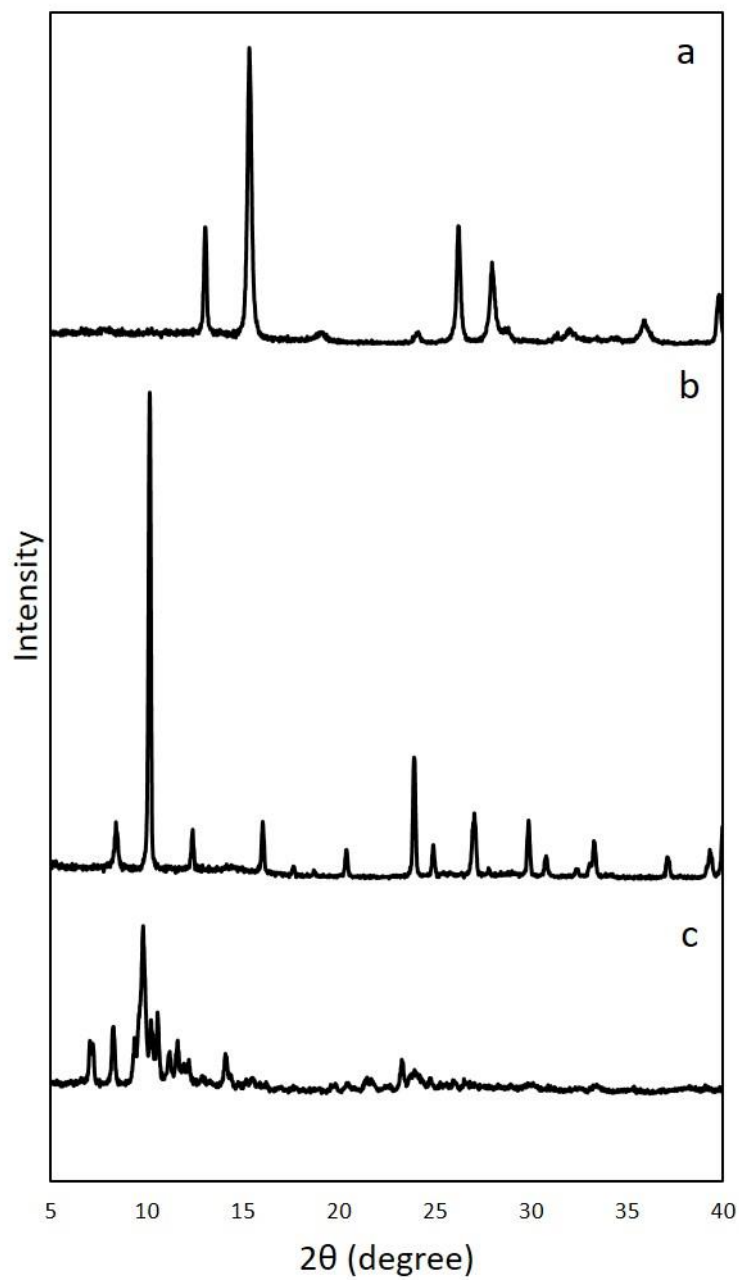


**Figure 7.1.** XRD patterns of the synthesized molybdenum oxides (a) MO (without surfactant) (b) MO-TMA1:2, and (c) MO-CTAB1:2.



The presence of surfactants CTAB and TMA in the synthesis medium dramatically influenced the crystalline phase of molybdenum oxide. Figures 7.1 b and c show XRD patterns of the samples prepared in the presence of these two surfactants with the surfactant/molybdenum molar ratio of 1:2 (denoted as MO-TMA1:2 and MO-CTAB1:2). The XRD pattern of MO-TMA (Figure 7.1b) indicates that the quaternary ammonium cation was incorporated into crystalline structure of the final product. TMA, also, affected the oxidation state of the formed molybdenum oxide. The peaks could be precisely indexed on monoclinic tetramethylammonium tetramolybdate,  $[\text{N}(\text{CH}_3)_4]\text{Mo}_4\text{O}_{12}$  (PDF no. 50-1901), and ammonium octamolybdate tetrahydrate  $(\text{NH}_4)_6\text{Mo}_8\text{O}_{27}\cdot 4\text{H}_2\text{O}$  (PDF no. 50-0607). The surfactant with longer organic chain, CTAB, directed the crystalline phase toward a multiphase structure. As seen in Figure 7.1c, it has much more peaks than the previous samples in  $2\theta$  less than  $15^\circ$ , which could be mainly ascribed to the crystalline phases of  $\text{MoO}_3$  (PDF no. 21-0569), ammonium molybdenum oxide hydrates  $(\text{NH}_4)_6\text{Mo}_7\text{O}_{24}\cdot 4\text{H}_2\text{O}$  (PDF no. 11-0071) and  $(\text{NH}_4)_4(\text{Mo}_8\text{O}_{24.8}(\text{O}_2)_{1.2}(\text{H}_2\text{O})_2)(\text{H}_2\text{O})_4$  (PDF no. 88-1326), and tetramethylammonium tetramolybdate  $[\text{N}(\text{CH}_3)_4]\text{Mo}_4\text{O}_{12}$  (PDF no. 50-1901). This multiphase is probably due to the cationic nature of CTAB during the synthesis reaction, which could be adsorbed by molybdenum oxide nuclei and afterward, it would detach at different times to form multiple phases.

Figure 7.2 shows SEM images of the synthesized materials prepared with and without the surfactants. Apart from 1:2, two other molar ratios of surfactant/molybdenum (1:3 and 1:4) were used in the synthesis to investigate the effects of the surfactant amounts on final morphology. The prepared samples are denoted as MO-CTAB1:4, MO-CTAB1:3, MO-TMA1:4, and MO-TMA1:3. SEM image of MO, synthesized without surfactant, (Figure 7.2a) demonstrates one-dimensional nanorods with a few micrometers length.

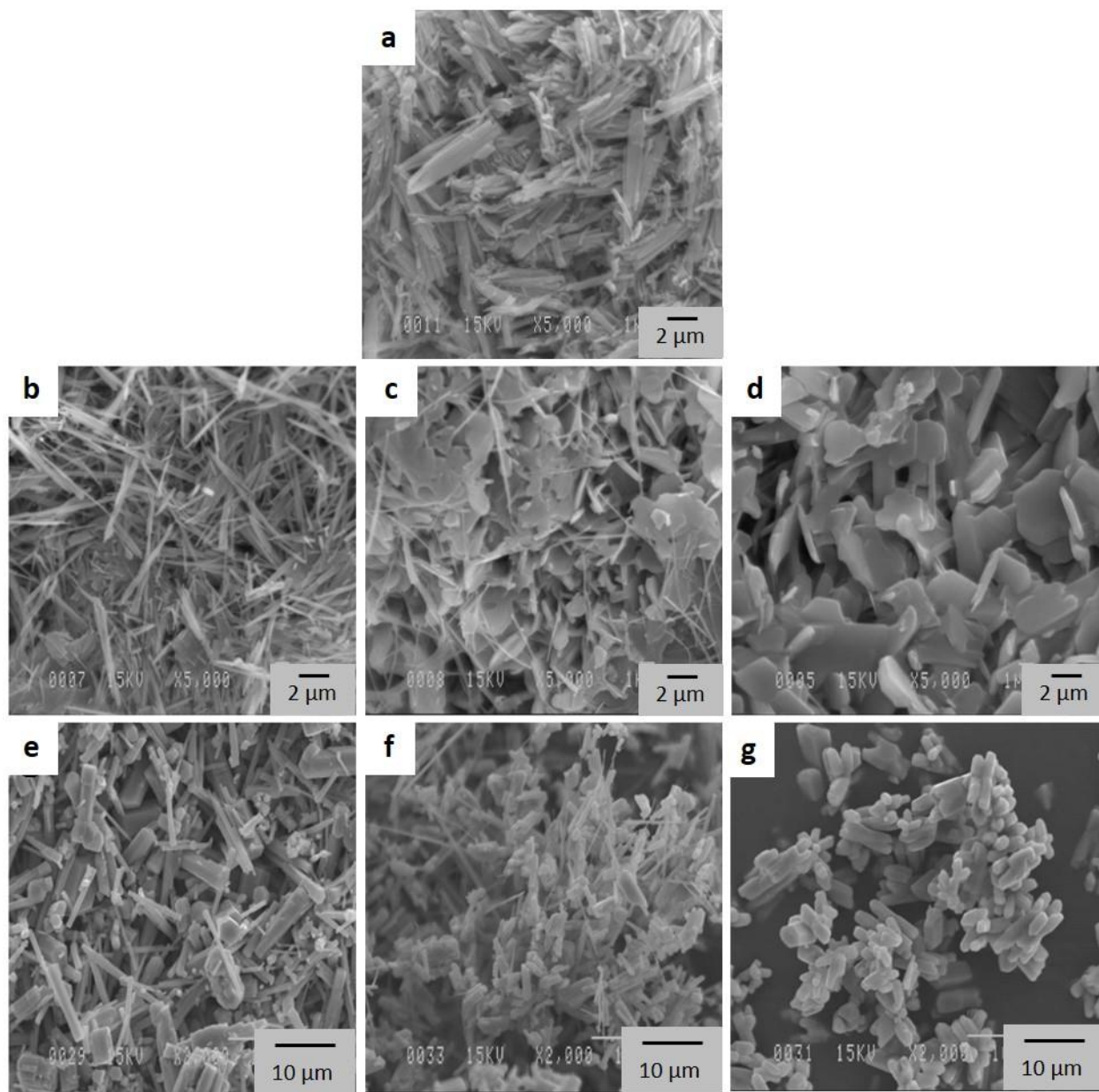


**Figure 7.2.** SEM images of the synthesized molybdenum oxides: (a) MO (b) MO-CTAB1:4, (c) MO-CTAB1:3, (d) MO-CTAB1:2, (e) MO-TMA1:4, (f) MO-TMA1:3, and (g) MO-TMA1:2.

Obviously, different sizes and morphologies were observed depending on the concentration as well as nature of the surfactant used (Figure 7.2 b-g). Lower amount of CTAB in MO-CTAB1:4 (Figure 7.2 b) did not change the morphology significantly; similar nanorods were obtained. Increasing CTAB content in MO-CTAB1:3, however, a heterogeneous mixture of nanorods and

microplatelet-like morphology was obtained (Figure 7.2 c), which became homogeneous microplatelets in MO-CTAB1:2. The effect of high concentration of CTAB is in good agreement with previous works, where stacked micro size of MoO<sub>3</sub> fibers and micro-ellipsoid structure of MoO<sub>3</sub> were predominant [390,391].

Using TMA in the synthesis considerably increased size of the product particles, leading to a heterogeneous mixture of microrods, which turned to agglomerated rods when concentration of TMA increased (Figure 7.2 e-g). By contrast to CTAB, the size of these hybrids particles containing TMA did not change considerably by changing the amount of TMA. From these studies, it can be observed that morphology of the particles has been influenced significantly by the nature of the surfactants.

Generally, the mechanism of MoO<sub>3</sub> formation follows the anisotropic growing of MoO<sub>6</sub> octahedral crystal nuclei as basic building unit of MoO<sub>3</sub> [392,393]. In absence of any surfactant in the synthesis medium, the growth along [010] direction is much more favored, and thus, results in formation of nanofiber, as shown in Figure 7.2 a. Although using a low amount of CTAB in MO-CTAB1:4 did not significantly change the morphology (Figure 7.2 b), further increasing of CTAB in MO-CTAB1:3 and MO-CTAB1:2 led to formation of an emulsion, highly likely because concentration of CTAB reached the critical micelle concentration (CMC). The lipophilic groups of micelles tend to move inward and hydrophobic groups outward. The concentration of CTAB up to 1:3 led to a stable spherical micelle and still generated thin fibers. However, the further increase of CTAB concentration more than CMC increased the deformation of micelle [392]. It has been reported that at higher concentrations of CTAB, the shape of micelles changes from sphere to prolate ellipsoid, and then the preferred orientation growth of MoO<sub>3</sub> is inhibited, resulting in the micro-ellipsoid structure [392]. The concentration of CTAB up to 1:3 led to both spherical and deformed micelles thus the material possesses both fibers and plates morphology in Figure 7.2 c. The highest concentration of CTAB generated homogeneous deformed micelles leading to only large plates in MO-CTAB1:2 (Figure 7.2 b). The use of TMA as a surfactant seems like it could not produce enough micelles and the concentration of TMA appears to have no effect on the size of particles. According to the literature, the Ostwald ripening mechanism [394] leads to the formation of hexagonal rods after growth, and TMA has not shown much effect and this was confirmed by XRD analysis (Figure 7.1 c).

FTIR analysis has been employed to identify the presence of surface functional groups on the catalyst. Figures 7.3 and 7.4 show the FTIR spectra of the samples prepared with CTAB and TMA, respectively. In both figures, FTIR spectra of the corresponding surfactant, as well as, MO sample (prepared without surfactant) have been also included to gain better interpretations.

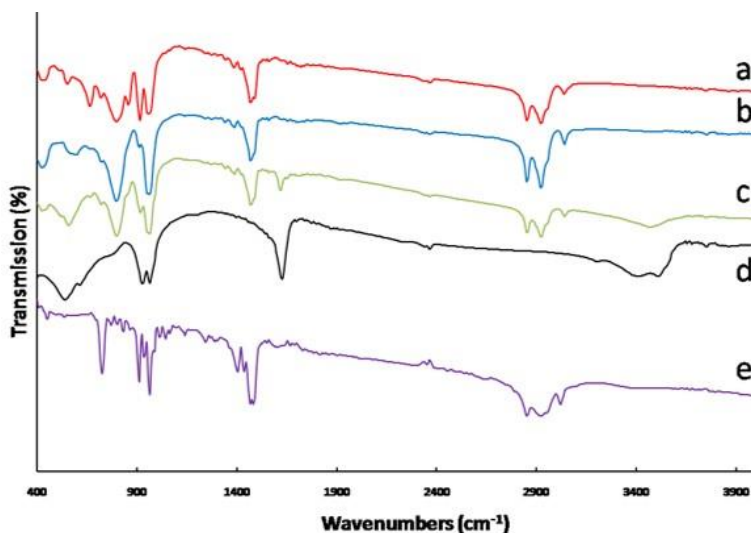


**Figure 7.3.** FTIR Spectra of the molybdenum oxides prepared with CTAB at various concentrations: (a) MO-CTAB1:2, (b) MO-CTAB1:3, (c) MO-CTAB1:4, (d) MO, and (e) CTAB.

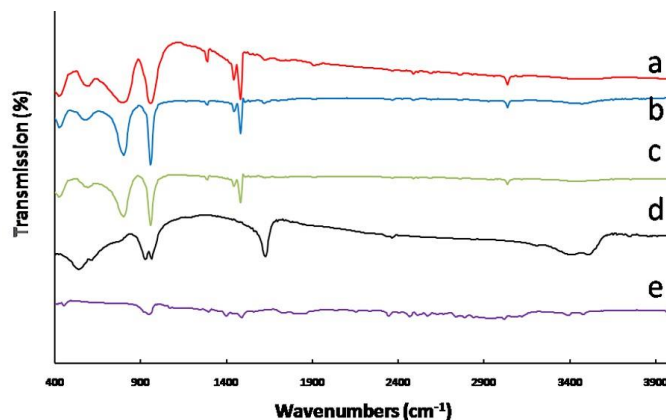


**Figure 7.4.** FT-IR Spectra of the molybdenum oxides prepared with TMA at various concentrations: (a) MO-TMA1:2, (b) MO-TMA1:3, (c) MO-TMA1:4, (d) MO, and (e) TMA.

Figure 7.3 shows two bands at 2920 and 2850 cm<sup>-1</sup> for the CTAB-containing samples (Figure 7.3 a-c), which are attributed to the characteristic peaks of symmetric and asymmetric C–

H stretching vibrations of methylene groups of CTAB. Moreover, the characteristic peak of angular deformation vibrations of methylene group was also observed at  $1475\text{ cm}^{-1}$  in these samples. These results were verified by the spectrum of pure CTAB (Figure 3e).

As seen in Figure 7.4, asymmetric and symmetric deformation modes pertaining to  $(\text{CH}_3)_3\text{N}^+$  of the head group of TMA appear at around  $1490$  and  $1390\text{ cm}^{-1}$ , according to the literature [390]. Pure TMA spectrum (Figure 7.4 e) shows the deformation vibrations of methyl groups at  $1490$  and  $1397\text{ cm}^{-1}$  and all other samples containing TMA confirm these characteristic peaks (Figure 7.4 a-c). Detailed analysis of spectrum of MO sample (Figure 7.3 d or 7.4 d) reveals that the characteristic peak of stretching vibrations of Mo-O appears at  $540\text{ cm}^{-1}$  [394,395,390], which was shifted to  $563$  and  $556\text{ cm}^{-1}$  in the presence of CTAB and to  $580\text{ cm}^{-1}$  in the presence of TMA (Figures 7.3 and 7.4). The stretching mode of Mo=O bands was located at  $965\text{ cm}^{-1}$  and  $934\text{ cm}^{-1}$  [396,397], and no peak was observed around  $995\text{ cm}^{-1}$  which is generally assigned to stretching vibrations of Mo-O-Mo. It is a characteristic of the orthorhombic phase of  $\text{MoO}_3$ .

The peaks observed at  $1630\text{ cm}^{-1}$  and  $3550\text{ cm}^{-1}$  were attributed to stretching and bending vibration of hydrogen bonded -OH groups, qualitatively confirming the presence of OH groups on the surface and water molecules adsorbed in the catalysts, which concur with the results of XRD analysis. Quantitative analysis of water contents of catalysts was performed by thermo-gravimetric analysis (TGA).

Figure 7.5 and 7.6 show TGA curves of the samples synthesized with CTAB and TMA, respectively. TGA curve of MO (without surfactant) (Figure 7.5 d or 7.6 c), shows a primary weight loss ( $\sim 12\%$ ) observed in the range of  $70$  to  $200\text{ }^\circ\text{C}$ , which corresponds to desorption of physically adsorbed water on  $\text{MoO}_3\text{-H}_2\text{O}$ . After  $200\text{ }^\circ\text{C}$  the weight of MO remained constant up to  $700\text{ }^\circ\text{C}$ , confirming the thermal stability of molybdenum oxide without any surfactant attached on its surface. Further heating after  $700\text{ }^\circ\text{C}$  led to a great weight loss not only for MO sample but also for the other samples, which is due to sublimation of molybdenum oxide that has been reported before [398].

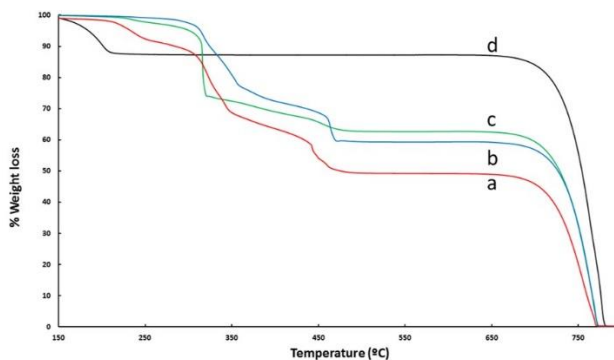


**Figure 7.5.** TGA curves of the molybdenum oxides prepared with different amounts of CTAB: (a) MO-CTAB1:2, (b) MO-CTAB1:3, (c) MO-CTAB1:4, and (d). MO.

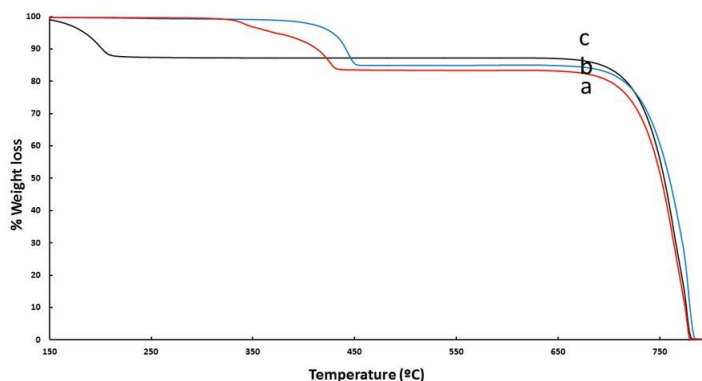


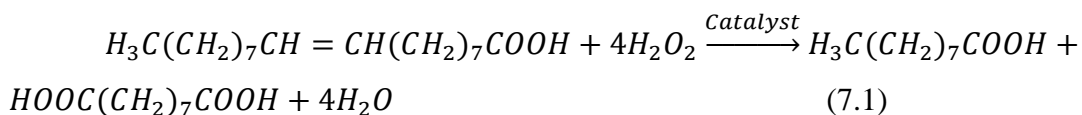
**Figure 7.6.** TGA curves of the molybdenum oxides prepared with different amounts of TMA: (a) MO-TMA1:2, (b) MO-TMA1:3, and (c) MO.

TGA curves of the samples containing CTAB (Figure 7.5 a-c) generally show lower weight losses compared to MO in the low-temperature region of  $< 200$  °C, which was attributed to the hydrogen bonded water molecules present in the crystalline phase; this assumption was confirmed by FTIR. The second weight loss observed at the range of 200-300 °C could be ascribed to decomposition of nitrates and ammonia compounds obtained from the surfactant. In addition, a third weight loss was obtained in high-temperature region ( $300 < T < 500$  °C), for which further differential thermal analysis (DTA) confirmed that it belongs to an exothermic interaction. This weight loss could be ascribed to removal or decomposition of  $\text{CTA}^+$  and elimination of bromide species during oxidation in air. The total amount of weight losses had a positive relationship with CTAB content in the samples; 50, 40, and 37 % weight losses were obtained for MO-CTAB1:2,

1:3, and 1:4, respectively. TGA curves of the samples with TMA (Figure 7.6) and their DTA analysis showed exothermic peaks between 300 and 450 °C corresponding to elimination of  $^+\text{N}(\text{CH}_3)_4$  group and bromide species. The weight losses during oxidation were between 16 and 17% which are much lower compared to those of the CTAB-capped samples. It could be due to the small molar weight of TMA (210.16 g/mol) compared to that of CTAB (364.45 g/mol).

### 7.3.2 Catalytic tests results

Catalytic activities of the surfactant-capped molybdenum oxide catalysts in oxidative scission of oleic acid have been investigated in a glass reactor equipped with condenser, thermocouple, and magnetic stirrer. A reaction was conducted without oleic acid to determine  $\text{H}_2\text{O}_2$  loss via catalytic or thermal decomposition and the loss was determined by titrimetry. For 4 h reaction at 85 °C, the loss of the oxidant was 26 %. Therefore, excess amounts of  $\text{H}_2\text{O}_2$  were used to complete the oxidation reactions (the molar ratio of  $\text{H}_2\text{O}_2$ /oleic acid used in the reaction was 11.1, which shows about 180% excess amount of  $\text{H}_2\text{O}_2$ , based on the stoichiometric reaction, Equation 7.1).



The first step of the reaction involves protonation of peroxo moiety on the catalyst to give surface peroxo groups. A yellow suspension was observed in the reaction solution, due to the formation of metal-peroxo complexes,  $-\text{MoO}(\text{O}_2)$  on surfaces of the surfactant-capped catalysts. Time-lapse observations of the reaction mixture, containing catalyst, oleic acid, hydrogen peroxide and tert-butanol, was recorded during the reactions over the catalysts to track changes that take place slowly over time (Figures S7.1 and S7.2, Supporting Information). Intriguingly, heterogeneity behavior of MO-CTAB1:3 catalyst was changed during the reaction; in the beginning of the reaction, the catalyst was a solid powder observable in the reaction mixture, which, upon heating to 85° C, turned into a homogeneous system. Afterwards, the reaction mixture remained as a clear solution until the end of the reaction. As soon as cooling down to room temperature, the catalyst started to precipitate (Figure S7.1), enabling self-separation and easy recovery of the catalyst. By contrast, all of the TMA containing catalysts kept their solid and heterogeneity natures during the reaction (Figure S7.2). This may be due to the structural differences between these two

surfactants; CTAB has a long hydrophobic chain of cetyl groups, which improves the hydrophobic-hydrophobic interaction between the surface of molybdenum oxide and oleic acid molecules and traps these molecules in the reaction medium resulting in enhancement of contacts between the reactants and active sites on the catalyst. The high dispersion of MO-CTAB1:3 catalyst in the reaction mixture, which arose from the surface organo-modification, created conditions similar to homogeneous catalysis. Moreover, the high concentration of hydrogen peroxide during the reaction results in rapid formation of metal-peroxo complexes and reinforcement of the emulsion, while at the end of the reaction, when a majority of H<sub>2</sub>O<sub>2</sub> has been consumed, the concentration of such complexes on the catalyst's surface drops resulting in precipitation of the catalyst.

Table 7.1 shows the conversion of oleic acid and yields of production of the desired products, azelaic and pelargonic acids, over different synthesized catalysts with H<sub>2</sub>O<sub>2</sub> as oxidant after 3.5 h reaction at 85 °C. The catalytic test results presented are the average of at least 3 runs over each catalyst. The first catalytic test was done without any catalyst (Table 7.1, entry 1), that gives very low conversion (26%) and yields of azelaic and pelargonic acids (6.4 and 6.8%, respectively). Using the catalyst without surfactant, MO, significantly increased the conversion (97%) and yields of azelaic and pelargonic acids (60 and 50%, respectively) (entry 2). The overwhelming majority of the organo-modified catalysts resulted in better efficiencies (entries 3-8). Ideally, oxidative cleavage of oleic acid should give similar yields of azelaic and pelargonic acids (1 mole of oleic acid into 1 mole of each product) based on the stoichiometric equation of the reaction (Equation 7.1). In practice, however, differences were obtained in the yields of these two products, which arise from non-ideality of the catalytic system, different decomposition rates of azelaic and pelargonic acids in the reaction medium, and presence of by-products.

**Table 7.1.** Catalytic tests results (conversion of oleic acid and yields of production of desired products).

Entry	Catalyst	Surfactant: Mo molar ratio	Conversion <sup>1</sup> (%)	Yield <sup>2</sup> of azelaic acid (%)	Yield <sup>2</sup> of pelargonic acid (%)
1	Without catalyst	-	26	6.4	6.8
2	MO	0	97	60	50
3	MO-CTAB1:4	1:4	100	78.2	61
4	MO-CTAB1:3	1:3	100	83	68



5	MO-CTAB1:2	1:2	100	70	55
6	MO-TMA 1:4	1:4	100	68	59
7	MO-TMA 1:3	1:3	100	67.4	60
8	MO-TMA 1:2	1:2	100	58	46

1. Reaction conditions: time: 3.5 h, temperature: 85 °C (bath temperature), solvent: tert-butanol, initial amounts of oleic acid: 1 g, t-butanol: 8 ml, H<sub>2</sub>O<sub>2</sub>: 4 ml, catalyst: 0.4 g.
2. Yield, in this work, is defined as the number of moles of a product formed per mole of oleic acid consumed

Use of the surfactants as capping agent increased both yields of azelaic and pelargonic acids. The maximum yields were achieved with MO-CTAB1:3 catalyst (entry 4), which produced 83 % azelaic and 68% pelargonic acids. Compared to the literature, these obtained yields are superior to what have been obtained by heterogeneous catalysts and are comparable with what homogeneous ones have shown. Table 7.2 lists the results of other works (all the heterogeneous catalysts reported so far, to the best of our knowledge, and some of the best homogeneous catalysts). The excellent catalytic activity of MO-CTAB1:3, as Table 7.2 implies, could be ascribed to the presence of multiple alkyl chains on the catalyst's surface, which improves the interactions of oleic acid with peroxo-molybdenum complexes formed by the reaction of H<sub>2</sub>O<sub>2</sub> with the particles surfaces.

**Table 7.2.** Comparison of catalytic efficiency of MO-CTAB1:3 with recent reported works in the literature.

Catalyst/ oxidant system	Reaction time and temperature	Conversion (%)	Yield <sup>1</sup> (%)	Reference <sup>2</sup>
Peroxo-tungsten complex PTA/H <sub>2</sub> O <sub>2</sub>	5h, 80 °C	-	PA: 82 AA: 79	[2] *
Polyoxomolybdate	5h, 90 °C	-	AA: 82	[3] *
RuCl <sub>3</sub> /NaIO <sub>4</sub>	8h, RT	-	PA: 98 AA 62	[58] *
H <sub>2</sub> WO <sub>4</sub> /H <sub>2</sub> O <sub>2</sub>	8h, 100 °C	-	PA 69 AA 92	[386] *
Tungsten oxide-SiO <sub>2</sub> / H <sub>2</sub> O <sub>2</sub>	1h, 130 °C	79	PA 36 AA 32	[48] #
Tungsten oxide/ H <sub>2</sub> O <sub>2</sub>	1h, 130 °C	56	PA 29 AA 30	[48] #
Chromium supported on MCM-41/O <sub>2</sub>	8 h, 80 °C	> 95	AA: 32.4 PA: 32.2	[339] #
Tungsten oxide/ H <sub>2</sub> O <sub>2</sub>	5 h, 120 °C	95	AA: 58 PA: 24	[399] #
H <sub>2</sub> O <sub>2</sub> /MO-CTAB1:3	3.5 h, °C	100	PA 68% AA 83%	This work #

1. AA: azelaic acid, PA: pelargonic acid.
2. \*: homogeneous catalysis, #: heterogeneous catalysis

### 7.3.3 Recyclability of the catalysts

Stability and consequently reusability of the catalyst, which are important parameters to scale up the process, were also investigated for the catalyst that gave the best efficiency (MO-CTAB1:3). The catalyst was conveniently recovered from the mixture of products after the reaction by simple centrifugation at high rpm. No significant loss of catalyst (or no significant leaching of Mo species to the reaction solution) was found, even after 4 cycles of catalytic reaction. Yield of weight recovery for all the catalysts after the first cycle was more than ~97% and loss of the CTAB-capped catalyst after 4 cycles obtained by ICP analysis was 9.4 wt%. This good recovery could be due to the protective role of the capping surfactant on the catalyst surface. Table 7.3 represents catalytic efficiencies obtained by catalyst MO-CTAB1:3 in the four performed reaction cycles, which shows insignificant activity loss. Yields of desired products slightly decreased during the cycles while the conversion was always the same. Comparing FTIR spectra of MO-CTAB1:3 before and after each cycle (Figure 7.7) does not show any notable difference, which proves stability of the CTAB capped on the catalyst's surface. Even after the fourth cycle, CTAB groups were still attached to the catalyst; all the characteristic peaks of alkyl group and molybdenum oxide remained after the cycles. The slight decrease in the yields may be due to the progressive detachment of CTAB and leaching of molybdenum oxide from the particle surface to the solution (leaching of Mo oxide: ~ 10% after 4 cycles of reaction). Furthermore, to verify that the reaction is truly heterogeneous and to investigate the possibility of leaching of Mo species in the reaction solution after removal of the catalyst, a catalytic test was performed with MoCTAB1:3 catalyst and stopped after 1 h of reaction, which showed 44% conversion and 28 and 21% yields of azelaic and pelargonic acids, respectively. After cooling down to room temperature the catalyst was removed, and the reaction solution was exposed to the reaction conditions for the remaining reaction time (2.5 h, at 85 °C). Although the conversion increased to 61%, the yields were negligibly changed (29 and 23% for azelaic and pelargonic acids, respectively), which could be well ascribed to the lack of catalyst. However, since the oxidant could alone cause the conversion of oleic acid (see Table 7.1 entry 1), the conversion was increased somewhat. From these results, it can be concluded that this new catalytic system displays high activity, good selectivity and environmentally benign

properties (using hydrogen peroxide instead of hazardous ozone) and the efficient reusability of the catalyst makes the process cost effective and eco-friendly.

**Table 7.3.** Catalytic efficiencies obtained by catalyst MO-CTAB1:3 in different reaction cycles.

Catalysts	Reaction cycle	Conversion <sup>1</sup> (%)	Yield <sup>2</sup> of azelaic acid (%)	Yield <sup>2</sup> of pelargonic acid (%)
MO-CTAB1:3	1	100	83	68
MO-CTAB1:3	2	100	80	65
MO-CTAB1:3	3	100	78	63
MO-CTAB1:3	4	99	77	61

1. Reaction conditions: time: 3.5 h, temperature: 85 °C (bath temperature), solvent: tert-butanol, initial amounts of oleic acid: 1 g, t-butanol: 8 ml, H<sub>2</sub>O<sub>2</sub>: 4 ml, catalyst: 0.4 g.
2. Yield, in this work, is defined as the number of moles of a product formed per mole of oleic acid consumed.

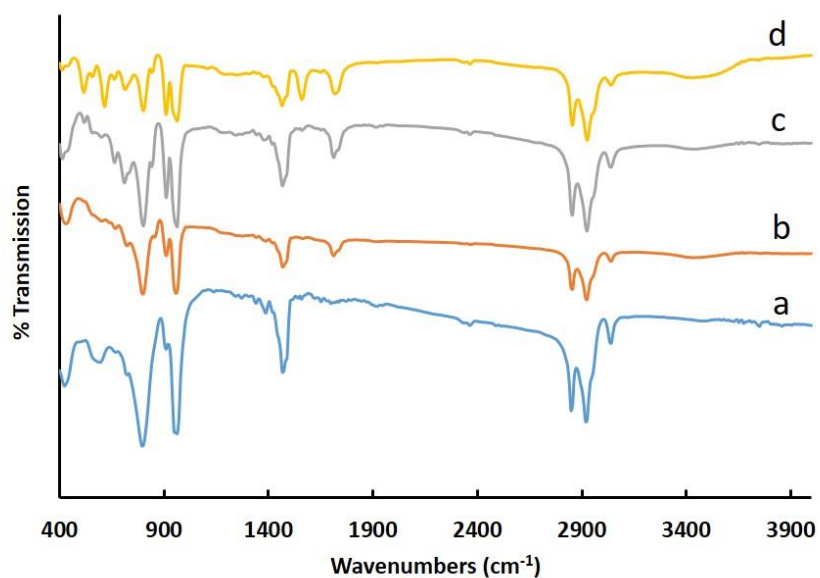


**Figure 7.7.** FT-IR Spectra of MO-CTAB1:3 catalyst after different reaction cycles: (a) after cycle 1, (b) after cycle 2, (c) after cycle 3, and (d) after cycle 4.

## 7.4 Conclusions

In summary, we have reported successful synthesis of surfactant-capped molybdenum oxide catalysts by simple oxidative dissolution method at 100 °C, which were characterized by different techniques including XRD, FTIR, TGA, and SEM analyses. CTAB and TMA were used

as surfactant to organo-modify surfaces of molybdenum oxides. The physicochemical analysis revealed that the morphology of the products strongly depends on the nature and concentration of capping agents. The synthesized surfactant-capped catalysts showed excellent catalytic efficiency in oxidative cleavage of oleic acid to mono and dicarboxylic acids. The highest efficiency was obtained for the CTAB-capped molybdenum oxide (with CTAB/Mo molar ratio of 1/3), resulting in full conversion of oleic acid and 83 and 68 % yields of production of azelaic and pelargonic acids, respectively. This catalyst exhibited convenient recovery, good stability, and steady reusability over recycling experiments without significant activity loss up to four cycles. Employing an environmentally benign oxidant, hydrogen peroxide, this catalytic system would open a new pathway for production of diacids and fuel components from renewable feedstock.

### **Funding**

This study was funded by Programme Canadien de Bourses de la Francophonie” (PCBF) and Nature Sciences and Engineering Research Council of Canada (NSERC) through an INNOV-UC Grant.

### **Acknowledgments**

This work was supported by the “Programme Canadien de Bourses de la Francophonie” (PCBF) and the Nature Sciences and Engineering Research Council of Canada (NSERC) through an INNOV-UC Grant. ASE thanks the Department of Chemical Engineering at Laval University for welcoming him as a visiting scientist during his stay in Canada. The authors would like to thank the industrial partners (Oleotek and SiliCycle Inc.) for stimulating discussions and comments.

## 7.5 Supporting Information



**Figure S7.1.** Time-lapse views of the reaction mixture in the presence of MO-CTAB1:3 catalyst: (a) beginning of the reaction, (b) during the reaction, and (c) end of the reaction.

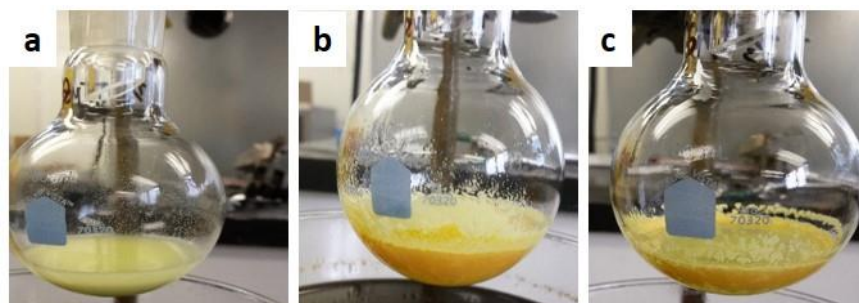


**Figure S7.2.** Time-lapse views of the reaction mixture in the presence of MO-TMA1:3 catalyst: (a) beginning of the reaction, (b) during the reaction, and (c) end of the reaction.